Muscarinic K^+ Channel in the Heart
Modal Regulation by G Protein βγ Subunits

Tatyana T. Ivanova-Nikolova, Emil N. Nikolov, Carl Hansen, and Janet D. Robishaw

From the Henry Hood MD Research Program, Department of Cellular and Molecular Physiology, Penn State College of Medicine, Danville, Pennsylvania 17822

ABSTRACT The membrane-delimited activation of muscarinic K^+ channels by G protein βγ subunits plays a prominent role in the inhibitory synaptic transmission in the heart. These channels are thought to be heterotetramers comprised of two homologous subunits, GIRK1 and CIR, both members of the family of inwardly rectifying K^+ channels. Here, we demonstrate that muscarinic K^+ channels in neonatal rat atrial myocytes exhibit four distinct gating modes. In intact myocytes, after muscarinic receptor activation, the different gating modes were distinguished by differences in both the frequency of channel opening and the mean open time of the channel, which accounted for a 76-fold increase in channel open probability from mode 1 to mode 4. Because of the tetrameric architecture of the channel, the hypothesis that each of the four gating modes reflects binding of a different number of Gβγ subunits to the channel was tested, using recombinant $G\beta_1\gamma_5$. $G\beta_1\gamma_5$ was able to control the equilibrium between the four gating modes of the channel in a manner consistent with binding of Gβγ to four equivalent and independent sites in the protein complex. Surprisingly, however, $G\beta_1\gamma_5$ lacked the ability to stabilize the long open state of the channel that is responsible for the augmentation of the mean open time in modes 3 and 4 after muscarinic receptor stimulation. The modal regulation of muscarinic K^+ channel gating by Gβγ provides the atrial cells with at least two major advantages: the ability to filter out small inputs from multiple membrane receptors and yet the ability to create the gradients of information necessary to control the heart rate with great precision.

KEY WORDS: signal transduction • guanine triphosphate binding proteins • muscarinic receptor • atrial myocytes

INTRODUCTION

The cardiac muscarinic inward rectifier potassium channels (K_{ACh} channels) are responsible for the acetylcholine- (ACh)[1] and adenosine-induced deceleration of the heart rate and atrioventricular conduction. When either m_2-muscarinic cholinergic or A_1-purinergic receptors are activated in cardiac atrial myocytes, they interact with heterotrimeric regulatory GTP-binding proteins (G proteins), promoting dissociation of the G proteins into a Gα-GTP subunit and a Gβγ complex. Once dissociated, both the Gα-GTP and Gβγ subunits proceed to regulate several effectors in the myocytes (Clapham and Neer, 1993). It is now well recognized that the Gβγ dimers confer the activation of the K_{ACh} channels (Reuveny et al., 1994; Wickman et al., 1994). At the same time, the Gα subunits are thought to interact with additional signaling constituents, the regulators of G protein signaling (RGS proteins), that stimulate the intrinsic GTPase activity of the Gα subunit, leading to rapid reassociation of the G protein heterotrimer and termination of the signal (Doupnik et al., 1997; Saitoh et al., 1997).

Several members of an expanding family of structurally related G protein–activated inward rectifiers (GIRKs) have been recently identified (Dascal et al., 1993; Kubo et al., 1993; Lesage et al., 1994; Doupnik et al., 1995). The cardiac K_{ACh} channels consist of two homologous subunits, GIRK1 and GIRK4 (also known as CIR) (Krapivinsky et al., 1995; Wickman et al., 1998), that are thought to form tetrameric structures with a $(GIRK1)_2(GIRK4)_2$ stoichiometry (Silverman et al., 1996; Tucker et al., 1996). Both GIRK1 and GIRK4 subunits are composed of two putative transmembrane domains, flanked by large hydrophilic NH_2- and COOH-terminal domains residing within the cell. These NH_2- and COOH-terminal regions of GIRK1 and GIRK4 are thought to be involved in Gβγ interactions to mediate channel activation (Takao et al., 1994; Dascal et al., 1995; Huang et al., 1995; Kunkel and Peralta, 1995; Huang et al., 1997).

While the structural domains involved in the Gβγ binding have been identified, the molecular mechanisms directing K_{ACh} channel gating upon Gβγ binding remain enigmatic. Previous electrophysiological studies

Address correspondence to Janet D. Robishaw, Henry Hood MD Research Program, Dept. of Cellular and Molecular Physiology, Penn State College of Medicine, Danville, PA 17822. Fax: 717-271-6701; E-mail: jdr@psghs.edu

[1]*Abbreviations used in this paper:* ACh, acetylcholine; GIRK, G protein–activated inward rectifiers.

have shown that the native cardiac K_{ACh} channels exhibit sigmoidal stimulus–response curves, suggesting cooperative binding of three or four Gβγ subunits to a single channel molecule (Ito et al., 1991, 1992). It has been further postulated that the function of the K_{ACh} channels is controlled by two independent mechanisms: a G protein–independent fast gating of the channel and a G protein–dependent slow transition from an unavailable to an available K_{ACh} channel state (Hosoya et al., 1996). Another intriguing possibility, however, is that Gβγ subunits may control the function of the K_{ACh} channel by governing the equilibrium between several functional modes of the channel. In fact, we have recently shown that multiple gating modes of the K_{ACh} channel do exist in the atrial myocytes of the bullfrog *Rana catesbeiana* (Ivanova-Nikolova and Breitwieser, 1997). Yet it remains to be determined whether the modal regulation of the K_{ACh} channel is evolutionarily conserved and, if so, how Gβγ subunits control the balance between the different functional states of the channel in mammalian systems.

To address these questions, we studied the interactions of Gβγ with the native K_{ACh} channels in atrial myocytes of the neonatal rat heart. First, we examined the K_{ACh} channel gating upon activation of muscarinic receptors in the atrial myocytes and identified the presence of four distinct patterns of K_{ACh} channel gating. The different gating modes were characterized by differences in both the frequency of channel opening and the mean open time of the channel, which accounted for a 76-fold increase in channel open probability from mode 1 to mode 4. Further, to reveal the mechanisms underlying modal behavior of the K_{ACh} channel, we reconstructed channel activation in excised membrane patches using purified recombinant $G\beta_1\gamma_5$. Surprisingly, in the presence of $G\beta_1\gamma_5$ alone, the four gating modes of the K_{ACh} channel differed only in the frequency of channel openings, while the mean open time of the channel remained the same. Finally, the analysis of the equilibrium among the functional modes of the channel at different $G\beta_1\gamma_5$ concentrations demonstrated that the four gating modes reflected binding of a different number of $G\beta_1\gamma_5$ subunits to four equivalent and independent sites in the channel protein complex.

MATERIALS AND METHODS

Isolation and Cell Culture of Neonatal Cardiac Myocytes

Viable atrial myocytes were obtained from 1–2-d-old Sprague Dawley rats by a trypsin/chymotrypsin/elastase dissociation procedure as described previously (Foster et al., 1990). The dissociated cells were centrifuged through Percoll step gradients to obtain cell preparations consisting of >94% myocytes. The myocytes were suspended in Modified Eagle's Medium containing 5% newborn calf serum and 0.1 mM 5-bromo-2′-deoxyuridine and were plated at a density of 10^5 cells/cm^2 on cover slips precoated with 0.1% gelatin. After overnight incubation, the cells were washed to remove nonadherent cells and cultured in a defined serum-free media for four additional days (Hansen et al., 1994).

Expression and Purification of G Protein Subunits

Procedures for construction and selection of recombinant Baculoviruses encoding various β or γ subunits of the G proteins have been described previously by Iniguez-Lluhi et al. (1992). cDNA containing the entire coding region for a particular subunit was transferred to the baculovirus expression vectors pVL1392 and pVL1393. Recombinant viruses were generated by cotransfection of *Spodoptera frugiperda* (Sf9) insect cells with the recombinant pVL1392 and pVL1393 transfer vectors along with mutant *Autographa californica* nuclear polyhedrosis virus, as described by the supplier (PharMingen, San Diego, CA). All recombinant viruses were plaque purified and were verified by their ability to direct the expression of the appropriate proteins, as detected by immunoblotting. $G_{i\alpha1}\beta_1\gamma_5$ heterotrimers containing a hexahistidine (H_6) tag inserted into the $G_{i\alpha1}$ were expressed in Sf9 cells as described (Kozasa and Gilman, 1995). H_6-tagged heterotrimers were solubilized by 0.5% Lubrol and purified by adsorption to an H_6-affinity nickel column. The $\beta_1\gamma_5$ dimers were then selectively eluted from the column using a HEPES buffer (pH 8) containing 0.03 mM $AlCl_3$, 50 mM $MgCl_2$, and 10 mM NaF. The elution of the $G\beta_1\gamma_5$ complex was monitored by immunoblotting, using β_1- and γ_5-specific antibodies. The $\beta_1\gamma_5$ dimers were further purified to homogeneity using Fast Protein Liquid Chromatography Mono Q column (Pharmacia LKB Biotechnology Inc., Piscataway, NJ). Purity of the final product was determined by sodium dodecyl sulfate (SDS)-PAGE and silver staining before use.

Electrophysiology

Single-channel currents through K_{ACh} channels were recorded from cell-attached and inside-out patches of atrial myocytes using standard high resolution patch-clamp method (Hamill et al., 1981). The membrane potential was zeroed with the following bath solution (mM): 150 KCl, 5 EGTA, 5 glucose, 1.6 $MgCl_2$, 5 HEPES, pH 7.4. Pipette solution contained (mM): 150 KCl, 1 $CaCl_2$, 1.6 $MgCl_2$, 5 HEPES, pH 7.4. Patch pipettes were made from borosilicate glass (World Precision Instruments, Inc., Sarasota, FL) on a Flaming Brown micropipette puller (Sutter Instruments, Co., Novato, CA) and firepolished on a microforge (Narishige Scientific Instrument Lab., Tokyo, Japan). The resistance of the patch pipettes (when filled with pipette solution) was 10–20 MOhm. Either acetylcholine or adenosine was added to the pipette solution to activate m_2-muscarinic or A_1-purinergic receptors, respectively. Currents were recorded with a Patch Clamp List-Medical EPC-7 amplifier (ALA Scientific Instruments Inc., Westbury, NY), additionally filtered at 2 kHz with an eight-pole Bessel filter (Frequency Devices Inc., Haverhill, MA) and the acquired data was stored on the hard disk of a computer. Data acquisition and analysis were performed using Digidata 1200 (Axon Instruments, Foster City, CA) supported by version 6.0 of pCLAMP software (Axon Instruments). Channel opening and closing transitions were identified with the half-amplitude threshold-crossing algorithm. Idealized records of the amplitudes, and channel open and close times, were generated by the FETCHAN Events List function. To determine the residence time of the K_{ACh} channel in the different gating modes, the continuous records were divided into consecutive segments, the frequency of apparent openings, *f*, was calculated for each segment and *f* histograms were generated for further analysis.

RESULTS

Evidence for the Presence of Different Functional States of the K_{ACh} Channels in the Neonatal Rat Cardiac Myocytes

We have previously demonstrated that upon activation of endogenous G proteins in frog atrial myocytes, the K_{ACh} channels exhibit bursting behavior, shifting between three predominant patterns of gating. They were termed low, medium, and high frequency modes, according to the frequency of channel openings during individual bursts (Ivanova-Nikolova and Breitwieser, 1997). Under basal conditions, infrequent, agonist-independent channel openings display exclusively a low frequency behavior, while a maximal activation of G proteins by GTPγS favors the high frequency behavior of the K_{ACh} channels. To test whether such a multistep activation of the K_{ACh} channel has been evolutionarily conserved as a signal transduction mechanism, we examined the gating behavior of K_{ACh} channels after m_2-receptor stimulation in rat neonatal atrial myocytes.

The individual K_{ACh} channels, activated in cell-attached configuration by 1 μM ACh, differed considerably in their gating behavior. One gating pattern was characterized by infrequent channel openings separated by long silent intervals, while a second one was dominated by the apparent clustering of openings into long bursts of activity. Fig. 1 provides an illustration of the differences between these patterns of gating. First, a comparison of the all-points histograms unveiled an order of magnitude difference in channel open probability, P_o. Second, a comparison of the open time distributions revealed a correlation between the proportion of brief and long K_{ACh} channel openings and the pattern of gating. In 10 cell-attached patches selected for analysis (no recordings with superimposing openings were accepted for this or the following types of analysis), a sum of two exponentials provided an adequate fit to the open time distributions. In addition, the time constants of both fast and slow exponential components were similar for different K_{ACh} channels and had values of ~1 and ~7 ms, respectively. The fractions of the histograms fitted by each of the two components, however, were different for the channels exhibiting the patterns of activity illustrated in Fig. 1, *A* and *B*. Thus, the changes in the kinetic behavior of the K_{ACh} channels were associated with both a change in the open probability and a shift from a brief open state to a long open state of the channel. These two observations provided a basis for classification of the K_{ACh} channel gating into functionally distinct modes. In bullfrog atrial myocytes, such classification was entirely based on analysis of channel gating within well defined individual bursts, assuming that each burst reflected a single event of interaction between the ion channel and Gβγ. In rat neonatal atrial myocytes, however, similar unambiguous division of the single channel records into bursts was not

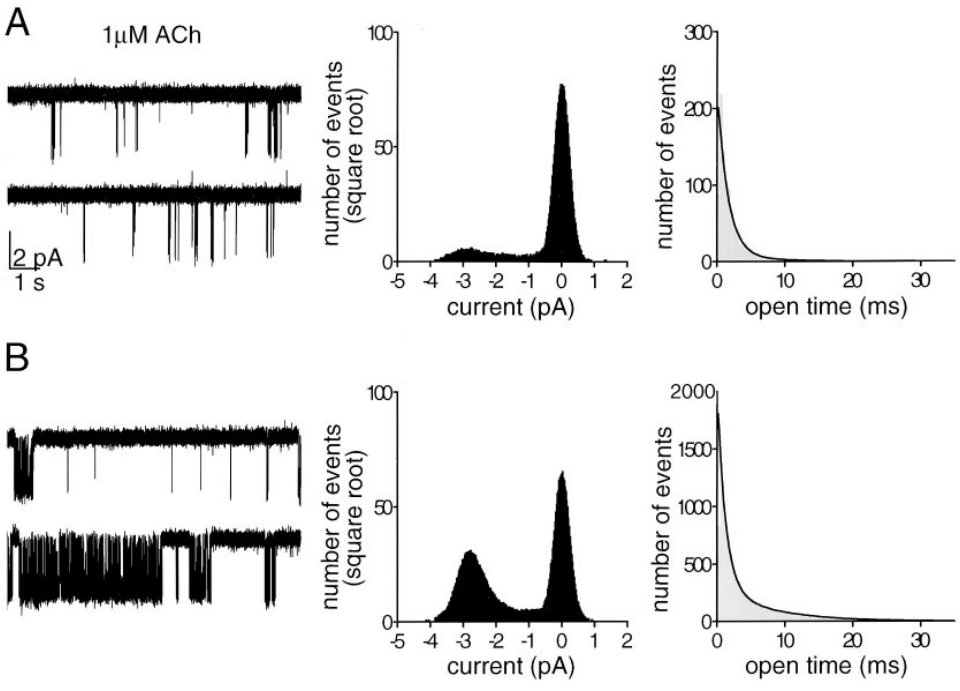

FIGURE 1. Heterogeneity of K_{ACh} channel gating in neonatal rat atrial myocytes. Two examples of single-channel activity recorded from cell-attached patches in the presence of 1 μM ACh are shown in *A* and *B* to illustrate the kinetic heterogeneity of channel gating encountered in our experiments. The membrane potential of the patch was held at −90 mV in both cases. In this and all figures, the downward deflections correspond to inward currents. All-points and open-time histograms generated from the data shown in *A* and *B* are presented on the right. The all-points histograms were fitted by the sum of two Gaussian functions to determine the channel open probability, P_o. The P_o value obtained from the 20-s record is 0.013 in *A* and 0.297 in *B*. The open time distributions were fitted by the sum of two exponential components. The time constants of the fast and slow components are τ_{o1} = 1.56 ms (83.6%) and τ_{o2} = 7.50 ms (16.4%) in *A* and τ_{o1} = 1.22 ms (52.1%) and τ_{o2} = 7.54 ms (47.9%) in *B*. The time constants of the fast and slow components showed little variations from one experiment to another; however, the relative areas under the individual exponents were different.

always possible. Therefore, we used a different approach for the classification of heterogeneous channel behavior into discrete gating modes. The continuous recordings were divided into consecutive, equally spaced time intervals and the channel behavior was assessed within these intervals. A duration of 400 ms was selected for the time intervals in this analysis based on the burst duration determined for the K_{ACh} channels exhibiting well-delineated bursting behavior. For each 400-ms data segment, the frequency of openings, *f*, and the probability of the channel being open, P_o, were calculated from the events list files and plotted vs. time. Fig. 2 illustrates this approach, using the two segments of K_{ACh} channel recordings shown in Fig. 1. Visual inspection of a large number of *f* and P_o plots verified that the selected time interval provided an adequate representation of the fluctuations in the K_{ACh} channel gating. Similar plots were generated from each of the 10 cell-attached recordings selected for analysis (total of 30 min of single-channel data). The *f* and P_o values within each 400-ms data segment were used to calculate the mean open time of the channel, t_{open}. The t_{open} values were further analyzed with regard to the frequency of openings to determine to what extent the changes in the frequency of gating could be correlated with changes in the mean open time of the K_{ACh} channel. The resulting t_{open}–*f* plot, shown in Fig. 3 *A*, revealed a multistep augmentation in the average t_{open} from 2.28 ± 0.10 ms at $f = 2.5$ Hz ($n = 999$ segments) to 6.24 ± 0.28 ms at frequencies above 47.5 Hz ($n = 231$ segments). Each statistically significant step in the t_{open} augmentation is indicated by an arrowhead in the t_{open}–*f* plot and presumably reflects a rather abrupt transition from one pattern of channel gating to another. The analysis of K_{ACh} channel gating, outlined above, identified transitions between four functional modes accessible to the channel upon activation of muscarinic receptors. A histogram of the frequency of openings was also generated to estimate the relative occupancy of different modes (Fig. 3 *B*).

Fig. 4 provides a direct comparison of several functional properties of the four K_{ACh} channel gating modes in neonatal rat atrial myocytes. Taken together, the differences in the frequency of channel openings and in the average open times account for significant changes in the open probability of the channel from one mode to the next. Thus, the mean open probability was ~20- and ~76-fold higher in modes 3 and 4, respectively, when compared with the open probability in mode 1. Such differences in the open probability would certainly have profound effects on the contributions of individual modes to the total current. Accordingly, modes 3 and 4 together contributed ~80% of the total current, although the K_{ACh} channels spent only 23% of their active time in these two modes.

These data indicate that the modal behavior of the K_{ACh} channels in neonatal rat atrial myocytes is qualitatively similar to the one described by us in bullfrog atrial myocytes (Ivanova-Nikolova and Breitwieser, 1997). The different number of gating modes identified in the rat myocytes (four, vs. three in the bullfrog myocytes) can be attributed to the elimination of mode 1 from the data selected for analysis in the bullfrog myocytes. In that case, individual bursts were defined as series of openings separated by closed intervals shorter than

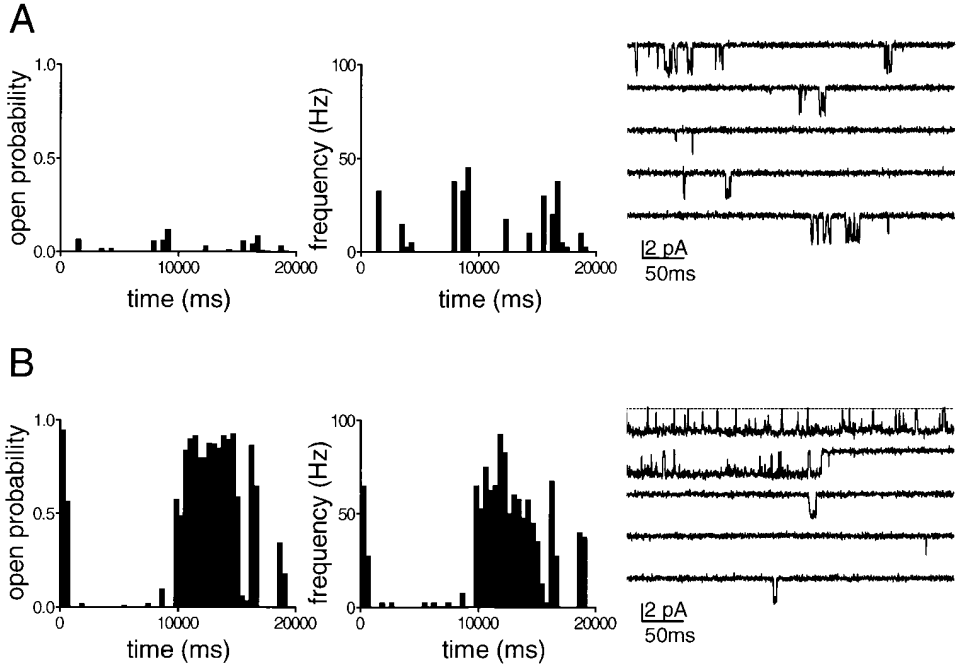

FIGURE 2. Approach for classification of the K_{ACh} channel gating. Continuous single-channel recordings were divided into consecutive, 400-ms segments and the channel open probability and the frequency of openings were determined for each individual segment. Plots of open probability and frequency of gating vs. time, derived from the continuous K_{ACh} channel records illustrated in Fig. 1, are shown for comparison in *A* and *B*. Expanded current traces from each of the two records (illustrating the first five 400-ms segments in which K_{ACh} channel activity was present) are shown on the right to reveal the kinetic behavior of the channel in greater detail.

some critical interval, usually between 120 and 140 ms. As a result, the singular events (separated by closed intervals longer than 140 ms) that delineate gating mode 1 were completely excluded from the analysis.

Regulation of Modal Behavior of the K_{ACh} Channels by G Protein βγ Subunits

To understand the mechanisms underlying the modal behavior of the K_{ACh} channel, we reconstructed channel activation in excised membrane patches using recombinant Gβγ. A major advantage of this approach over receptor-mediated activation of the K_{ACh} channel is that it provides a strictly controlled environment, abolishing potential contributions of intermediate signaling molecules to the K_{ACh} channel–Gβγ interactions. Since the composition of the Gβγ involved in the physiological regulation of the K_{ACh} channel is unknown, we selected the $G\beta_1\gamma_5$ isoform for our experiments, based on its relative abundance in the heart (Hansen et al., 1995). $G\beta_1\gamma_5$ dimers, expressed and purified from Sf9 cells, as previously described by Kozasa and Gilman (1995), were applied to activate directly the K_{ACh} channels in inside-out membrane patches excised from the rat atrial myocytes. Fig. 5 illustrates the activity recorded from the same K_{ACh} channel in a cell-attached patch in the presence of 1 μM adenosine (*A*), upon patch excision in GTP-free solution (*B*), and after application of 0.6 and 1.5 nM $G\beta_1\gamma_5$ (*C* and *D*, respectively). Nanomolar concentrations of $G\beta_1\gamma_5$ activated the K_{ACh} channels in a concentration-dependent manner similar to that reported by Wickman et al. (1994). The activation of the K_{ACh} channels developed over the course of 2–11 min after $G\beta_1\gamma_5$ application and was sustained during continued presence of $G\beta_1\gamma_5$. The gating behavior of the individual K_{ACh} channels remained heterogeneous even under such strictly controlled conditions, suggesting that the heterogeneity in the channel gating is an intrinsic property of K_{ACh} channel–Gβγ interactions.

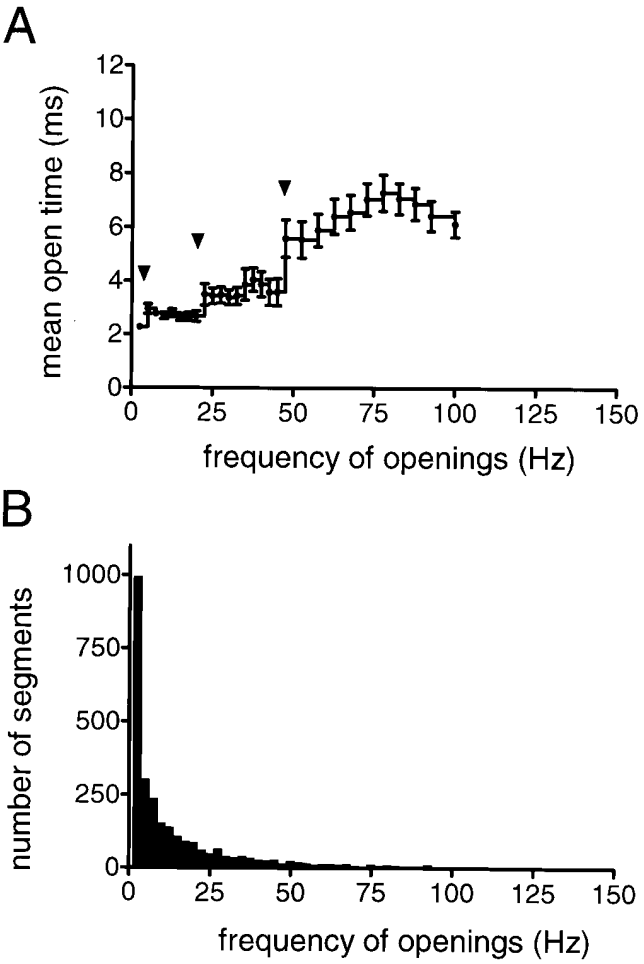

FIGURE 3. Segregation of K_{ACh} channel behavior into distinct gating modes. (*A*) The mean open time of the channel, t_{open}, is plotted as a function of the frequency of channel openings, *f*. The t_{open} value within each 400-ms data segment was calculated from the *f* and P_o values within the same segment. The t_{open} estimates were compiled from a total of 30 min of single-channel data recorded from 10 different cell-attached patches in the presence of 1 μM ACh, and the mean t_{open} value for a particular *f* population was determined. For the frequencies above 47.5 Hz, where the number of data segments was relatively small, the mean t_{open} value for each frequency, *f*, was averaged over a 5-Hz interval ($f \pm 2.5$ Hz). The arrowheads in the t_{open}–*f* plot indicate the statistically significant augmentations in the mean t_{open} value and presumably reflect the transitions from one pattern of K_{ACh} channel gating to another. (*B*) Histogram of frequencies of openings generated from the same set of data shown in *A*.

To reveal the source of this heterogeneity, the K_{ACh} channel gating in the presence of $G\beta_1\gamma_5$ was subjected to the same analysis routine described for analysis of the data recorded upon muscarinic receptor stimulation. The unitary currents through K_{ACh} channels activated by different concentrations of $G\beta_1\gamma_5$ were recorded for 20–30 min after the initial time interval required for incorporation of $G\beta_1\gamma_5$ in the membrane. The continuous single-channel recordings were divided into consecutive 400-ms segments, and three parameters, *f*, P_o, and t_{open}, were calculated for each data segment. The results from the analysis were then combined to generate a t_{open}–*f* plot and a frequency histogram for each individual experiment. Fig. 6 illustrates the t_{open}–*f* plots and the *f* histograms obtained from the experiment with the two different $G\beta_1\gamma_5$ concentrations, shown in Fig. 5, *C* and *D*.

The comparison of the t_{open}–*f* plots obtained at different $G\beta_1\gamma_5$ concentrations (ranging from 0.15 to 12 nM) with the t_{open}–*f* plot in Fig. 3 *A* revealed a key difference in the function of the K_{ACh} channels activated by $G\beta_1\gamma_5$ alone. While the mean open time of the receptor-activated channels underwent synchronized changes with the increase in the frequency of gating, the mean open time of $G\beta_1\gamma_5$-activated channels ($t_{open} = 1.86 \pm 0.09$

ms, $n = 10$) was unaffected by the frequency of gating (Fig. 6 *A*). Such a difference in the gating of receptor-activated and $G\beta_1\gamma_5$-activated K_{ACh} channels suggests that a combination of molecular interactions might contribute to the phenomenon of modal behavior. Given the ability of GIRK1 subunits of the K_{ACh} channel to bind $G\alpha_i$ to a binding site different from that for $G\beta\gamma$ (Huang et al., 1995), one intriguing scenario is that binding of both $G\alpha_i$ and $G\beta\gamma$ to the K_{ACh} channel is necessary to achieve the augmentation of t_{open} found after muscarinic receptor activation. Alternatively, different subclasses of $G\beta\gamma$ might exert different effects on the K_{ACh} channel regulation and the method outlined in the present work is sensitive enough to capture the distinctions between channel gating in the presence of $G\beta_1\gamma_5$ and in the presence of the unidentified, but hypothetically distinct, $G\beta\gamma$ released upon muscarinic receptor stimulation. Further studies will be required to distinguish between these two possibilities.

At the same time, the comparison of the frequency distributions obtained at different $G\beta_1\gamma_5$ concentrations (Fig. 6 *B*) revealed that the increases in $G\beta\gamma$ concentrations are translated into increases in the frequency of K_{ACh} channel openings. These distributions should consist of a sum of geometric components, and the number of components should reflect the number of conducting conformations of the channel (Colquhoun and Hawkes, 1981, 1983). We therefore used the geometric components in the *f* histograms to classify the gating behavior of $G\beta_1\gamma_5$-activated channels into distinct modes. In the presence of 0.15 nM $G\beta_1\gamma_5$, a single geometric component was sufficient to fit the *f* histograms, while a sum of up to four geometric components was required for the adequate fit of the data generated in the presence of higher $G\beta_1\gamma_5$ concentrations. The mean frequencies of the first through fourth components showed little variations from one K_{ACh} channel to another and averaged 2.2 ± 0.2 Hz ($n = 24$), 12.7 ± 0.6 Hz ($n = 20$), 33.6 ± 1.9 Hz ($n = 18$), and 65.0 ± 4.2 Hz ($n = 8$), respectively. These values are similar to the frequencies found for modes 1–4 of the receptor-activated K_{ACh} channels in the atrial myocytes (see Fig. 4 for comparison). Accordingly, with regard to the frequency of openings, the $G\beta_1\gamma_5$-activated K_{ACh} channels behaved in a manner approaching that of the receptor-activated channels, converting between four functional modes.

On the basis of these results, we proposed that binding of a different number of $G\beta\gamma$ subunits to four $G\beta\gamma$-binding sites in the tetrameric K_{ACh} channel structure gives rise to its four functional modes. For simplicity, we further assumed that the four $G\beta\gamma$-binding sites are functionally equivalent and independent. These assumptions imply that the four sites have the same binding affinity for $G\beta\gamma$, and that $G\beta\gamma$ binding to one site is not affected by the $G\beta\gamma$ occupancy of the remaining sites. Such a simple model predicts that the probability of observing each gating mode is given by the binomial distribution $[N!/k!(N - k)!]P^k(1 - P)^{N-k}$, where N is the total number of $G\beta\gamma$-binding sites, k is the number of the occupied binding sites, and P is the probability that one of the four $G\beta\gamma$-binding sites is occupied. To test this prediction, we quantified the equilibrium among the four gating modes at different $G\beta\gamma$ concentrations. The equilibrium probability (or relative occupancy) of different modes was estimated from the fraction of the total *f* histogram fit by the corresponding geometric component. In experiments using the same concentrations of $G\beta_1\gamma_5$, some variations in the relative occupancy of different modes were observed. These variations can be explained by differences in the probability of $G\beta\gamma$ binding, *P*, and can be attributed either to a different amount of $G\beta_1\gamma_5$ incorporated in the membrane or to a different binding affinity of the channel for $G\beta_1\gamma_5$. Therefore, in each experiment, the probability of $G\beta\gamma$ binding was calculated from the fraction of the *f* histogram fit by the first geometric component and the relative occupancy of different gating modes

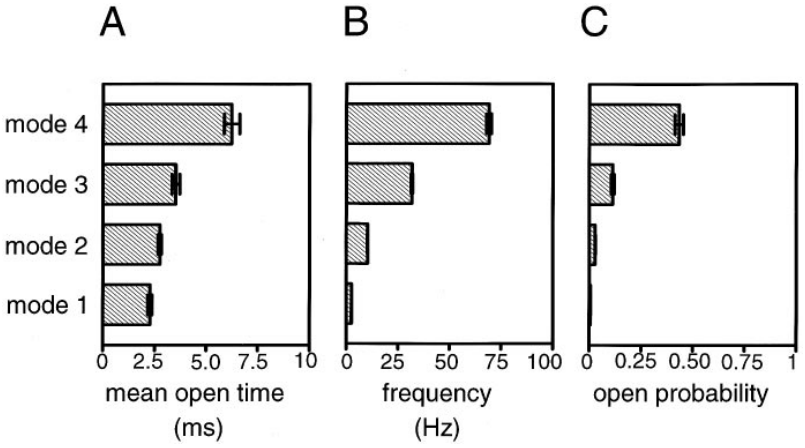

FIGURE 4. Properties of the four gating modes of the m_2 receptor-activated K_{ACh} channel. Three different parameters: mean open time (*A*), frequency of channel openings (*B*), and mean open probability (*C*) were evaluated with regard to modal behavior of the channel after muscarinic receptor stimulation. The values for the mean open time of each gating mode are: $t_{1open} = 2.28 \pm 0.10$, $t_{2open} = 2.75 \pm 0.08$, $t_{3open} = 3.53 \pm 0.19$, and $t_{4open} = 6.24 \pm 0.38$ ms. The values for the frequency of channel openings are: $f_1 = 2.5$, $f_2 = 10.3 \pm 0.1$, $f_3 = 31.7 \pm 0.3$, and $f_4 = 69.1 \pm 1.2$ Hz. The values for the mean open probability are: $P_{o1} = 0.0057 \pm 0.0003$, $P_{o2} = 0.0281 \pm 0.0010$, $P_{o3} = 0.1128 \pm 0.0065$, and $P_{o4} = 0.4341 \pm 0.0195$. Data are mean ± SEM ($n = 231$–1,116).

was examined as a function of Gβγ binding to the channel, rather than as a function of Gβγ concentration. The corresponding plot from this analysis is shown in Fig. 7 and verifies that the equilibrium probability of each mode is binomially distributed as predicted by the model. In this way, the analysis of the equilibrium among the four K_{ACh} channel functional states in the presence of $G\beta_1\gamma_5$ predicts the existence of four equivalent and independent Gβγ binding sites in the channel structure.

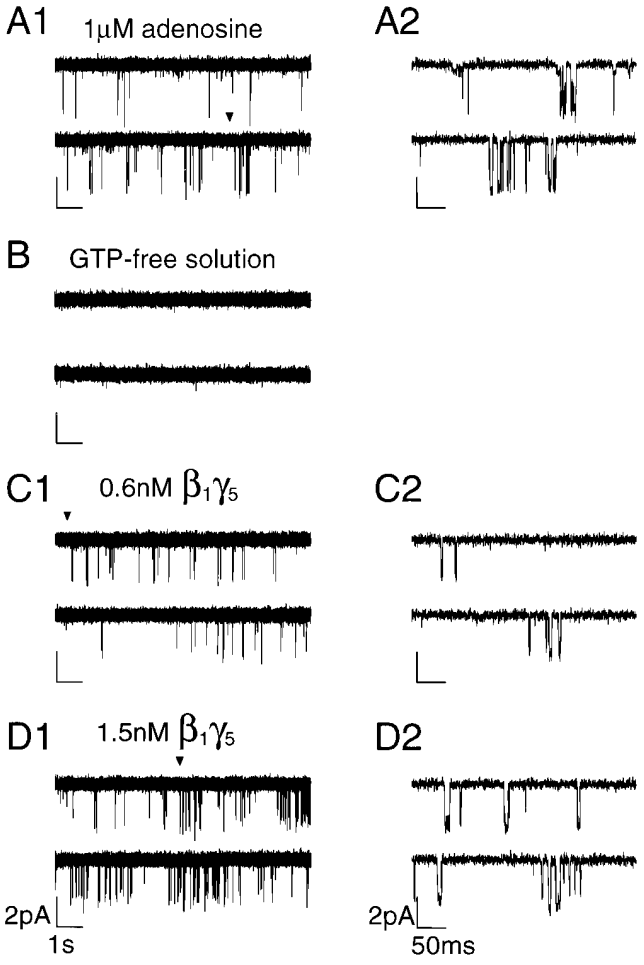

FIGURE 5. Activation of the K_{ACh} channels by recombinant $G\beta_1\gamma_5$. (*A1*) Representative single-channel activity recorded in cell-attached configuration from an atrial myocyte in the presence of 1 μM adenosine. The membrane potential was clamped at −90 mV. (*A2*) Part of the trace in *A1* (*arrowhead*) has been expanded to show the transitions between the closed and open states of the channel with a higher resolution. (*B*) Channel activity disappeared after the patch excision in GTP-free solution. The membrane potential continued to be clamped at −90 mV for the entire experiment. (*C–D*) Application of nanomolar concentrations of $G\beta_1\gamma_5$ (0.6 nM in *C1* and 1.5 nM in *D1*) restored the channel activity in a concentration-dependent manner. Extended current traces starting at the points indicated by the arrowheads in *C1* and *D1* are shown on the right in *C2* and *D2*, respectively.

It is interesting to note that in a small subset of $G\beta_1\gamma_5$ experiments (3 of 27), the mean frequencies of gating for each mode deviated by a factor of ~2 from the values estimated for m_2 receptor-activated K_{ACh} channels. In that case, the mean frequencies of the four modes were $f_1 = 3.7 \pm 0.3$, $f_2 = 21.4 \pm 1.1$, $f_3 = 54.7 \pm 1.9$, and $f_4 = 104.5 \pm 5.6$ Hz, while the conductance and the mean open time of these channels were similar to those determined for the rest of the $G\beta_1\gamma_5$-activated channels. Such differences in the channel gating, although infrequent, point to certain structural variability among native K_{ACh} channels in the heart. Evidently, a combination of K^+ channels susceptible to Gβγ regulation shapes the responsiveness of the atrial myocytes to G protein activation and the basic approach for classification of the K_{ACh} channel gating outlined in the present work creates a sensitive tool for capturing the functional variety among these channels.

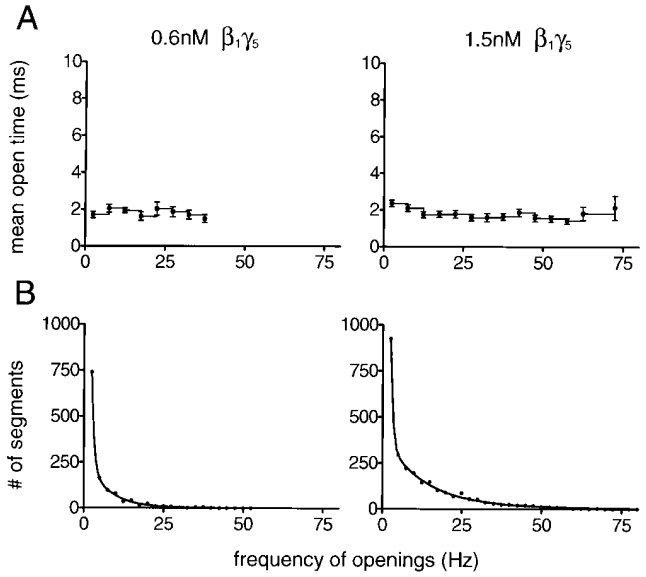

FIGURE 6. Modal classification of K_{ACh} channel gating in the presence of $G\beta_1\gamma_5$. (*A*) The t_{open}–f plots were generated from the analysis of the data illustrated in Fig. 5, *C* and *D*. In the presence of $G\beta_1\gamma_5$, the mean open time of the K_{ACh} channel was independent of the frequency of channel gating and approached the t_{open} value estimated for gating mode 1 of receptor-activated channels. (*B*) Histograms of frequencies of openings are shown for the experiments illustrated in *A*. The histogram shown at left corresponds to $G\beta_1\gamma_5$ concentration of 0.6 nM, whereas the histogram shown at right corresponds to $G\beta_1\gamma_5$ concentration of 1.5 nM. Both histograms were fitted by the sum of three geometrics (Colquhoun and Hawkes, 1981): $P(f) = a_1\mu_1^{-1}(1-\mu_1^{-1})^{f-1} + a_2\mu_2^{-1}(1-\mu_2^{-1})^{f-1} + a_3\mu_3^{-1}(1-\mu_3^{-1})^{f-1}$ (*continuous line*). The mean frequency values and the relative areas of different components are $\mu_1 = 1.4$ Hz (73.2%), $\mu_2 = 6.9$ Hz (23.5%), and $\mu_3 = 17.6$ Hz (3.3%) at 0.6 nM $G\beta_1\gamma_5$; and $\mu_1 = 1.3$ Hz (54.9%), $\mu_2 = 12.6$ Hz (35.5%), and $\mu_3 = 37.0$ Hz (9.6%) at 1.5 nM $G\beta_1\gamma_5$. The proportion of high frequency data segments consistently increased with $G\beta_1\gamma_5$ concentration.

DISCUSSION

The results outlined in the present work characterize the mechanism of membrane-delimited activation of muscarinic K^+ channels by Gβγ subunits in neonatal rat atrial myocytes and render an important clue to understanding the principles underlying the specificity of Gβγ-mediated signaling in general. These two aspects of our findings will be discussed below.

Mechanism of Gβγ Regulation of K_{ACh} Channels

Activation of K_{ACh} channels by acetylcholine and adenosine in sinoatrial nodal cells and atrial myocytes modulates both heart rate and cardiac contractility. The channel activation is brought about by a pertussis toxin–sensitive G protein (Breitwieser and Szabo, 1985; Pfaffinger et al., 1985) in a membrane-delimited manner (Soejima and Noma, 1984), using the G protein βγ subunits as direct information carriers between the membrane receptors and the K_{ACh} channels (Reuveny et al., 1994; Wickman et al., 1994). Because of their significance in the regulation of the heart function, K_{ACh} channels have been extensively studied at both whole-cell and single-channel levels (for review see Kurachi, 1995), yet the molecular mechanism underlying Gβγ–K_{ACh} channel interactions remains obscure. The only available functional model for G protein activation of the K_{ACh} channel was based on data from spectral analysis of current fluctuations at different GTP concentrations (Hosoya et al., 1996). In that case, the spectral analysis identified transitions only between two closed (C_1 and C_2) and one open (O) state of the K_{ACh} channel. Accordingly, the proposed model was based on two independent processes: a GTP-independent fast gating ($C_2 \leftrightarrow C_1 \leftrightarrow O$) and a slow, GTP-dependent transition (not detected in the power spectra) between unavailable and available channel states. Our recent single-channel analysis of the K_{ACh} channel regulation, however, clearly indicated that the channel activity is much more complex than previously thought and this activity is distributed between several gating modes (Ivanova-Nikolova and Breitwieser, 1997). To understand the mechanisms underlying such modal behavior of the K_{ACh} channel, in the present study, we performed an extensive single-channel analysis of the activation of the native K_{ACh} channel by recombinant $G\beta_1\gamma_5$ subunits. On the basis of this analysis, we formulated an alternative model of Gβγ–K_{ACh} channel interactions in which binding of a different number of Gβγ subunits to four Gβγ-binding domains in the K_{ACh} channel structure gives rise to four conducting conformations of the protein complex, linked in a dynamic equilibrium by the Gβγ concentration.

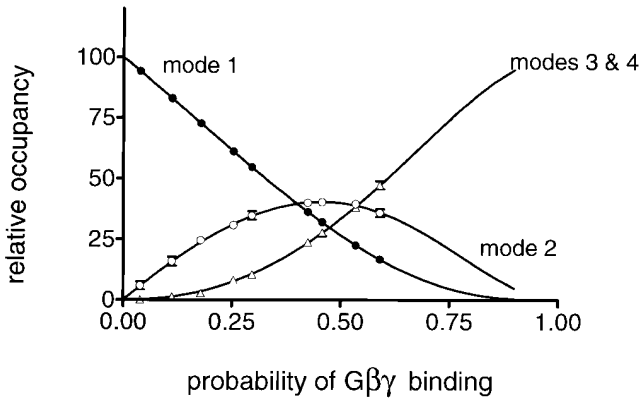

FIGURE 7. Modal equilibrium of $G\beta_1\gamma_5$-activated K_{ACh} channels. For each individual $G\beta_1\gamma_5$ experiment, the relative occupancy of different gating modes was estimated from the fraction of the *f* histogram fit by the corresponding geometric component. In some *f* histograms, the components representing gating modes 3 and 4 were too small to be accurately distinguished from each other and, therefore, the sojourns of the channel to these modes are jointly represented. In each experiment, the probability of $G\beta_1\gamma_5$-binding, *P*, was calculated from the relative occupancy of mode 1, $\tilde{\delta}_1$, according to the equation $\tilde{\delta}_1 = 4P(1 - P)^3/[1 - (1 - P)^4]$, as a standardization procedure. The solid lines represent the predicted occupancy of the different gating modes for a model assuming independent and equivalent binding of a different number of Gβγ subunits to four binding sites in the channel structure. The symbols and error bars are the mean values ± SEM of two to four separate experiments.

The heterogeneity of the K_{ACh} channel gating is a major obstacle in the interpretation of the single-channel recordings from both receptor- and $G\beta_1\gamma_5$-activated channels. Therefore, in the present study, we initially developed a basic approach for classification of the K_{ACh} channel gating into functionally distinct modes. The method is sensitive enough to capture subtle changes in the K_{ACh} channel regulation and greatly simplifies the kinetic analysis of the data. The analysis routine is based on fragmentation of continuous single-channel recordings into consecutive, equally spaced segments and subsequent characterization of the channel gating within individual segments. The characterization of channel gating combines the analysis of three different parameters: the frequency of openings, the probability of the channel being open, and the mean open time of the channel. The results from this analysis were then compiled to generate the frequency histograms and t_{open}–*f* plots as final readouts that convey the information about the dynamics of the K_{ACh} channel–Gβγ interactions.

In the present work, this method was successfully applied to classify the K_{ACh} channel gating into functionally distinct modes either by the appearance of several kinetic components in the frequency distributions, or by the orchestrated augmentations of K_{ACh} channel open time within the t_{open}–*f* plots. Two different series of experiments, one of which conserved the integrity of transduction cascade from the activation of muscarinic

receptors to the activation of the K_{ACh} channels, and another in which K_{ACh} channel activation was brought about solely by purified recombinant $G\beta_1\gamma_5$, indicated the presence of four functional modes of the channel. Remarkably, the two series of experiments yielded similar values for the predominant frequencies of channel openings within different gating modes. The values for the m_2 receptor-activated channels were: $f_{1ACh} = 2.5$, $f_{2ACh} = 10.3 \pm 0.1$, $f_{3ACh} = 31.7 \pm 0.3$, and $f_{4ACh} = 69.1 \pm 1.2$ Hz, while the values for the $G\beta_1\gamma_5$-activated channels were: $f_{1G\beta\gamma} = 2.2 \pm 0.2$, $f_{2G\beta\gamma} = 12.7 \pm 0.6$, $f_{3G\beta\gamma} = 33.6 \pm 1.9$, and $f_{4G\beta\gamma} = 65.0 \pm 4.2$ Hz. Thus, our analysis identified the frequency of channel openings as a principal parameter in the classification of the K_{ACh} channel activity into distinct gating modes.

Intriguingly, $G\beta_1\gamma_5$ alone was not able to reproduce the augmentation in the mean open time of the K_{ACh} channel in modes 3 and 4 associated with the channel activation through muscarinic receptors (Fig. 3 *A*). One possible reason for this could be that the unidentified Gβγ subunits released upon muscarinic receptor stimulation are structurally different from $G\beta_1\gamma_5$ and the active conformations of the channel vary depending on different Gβγ combinations. Alternatively, the augmentation in the mean open time could be regulated by different structural domains of the channel molecule and might require the binding of the Gα subunit to the channel. Validation of these possibilities requires direct experiments, which are currently under way.

Nevertheless, $G\beta_1\gamma_5$ was able to govern the equilibrium between the four functional modes of the channel. Multiple biochemical mechanisms might underline the modal behavior of the K_{ACh} channels. Any hypothetical mechanism, however, should take into consideration two important structural characteristics of the channel: its tetrameric structure (Silverman et al., 1996; Tucker et al., 1996) and the presence of numerous Gβγ-binding domains in the channel complex. Because of its simplicity, we considered a paradigm in which binding of increasing numbers of Gβγ subunits to four equivalent and independent positions in the channel protein complex would give rise to four distinct conformational states of the K_{ACh} channel. As long as the four gating modes of the channel can be regarded as reporters of such different conformational states, this paradigm predicts the probability of observing each gating mode as a function solely of the probability that one of the four Gβγ-binding sites is occupied, *P*. In this case, the probability function of each gating mode should follow the binomial distribution,

$$P_k = [N!/k!\,(N-k)!]\,P^k\,(1-P)^{N-k}, \qquad (1)$$

for binding of one, two, three, or four Gβγ subunits to four Gβγ-binding sites on the tetrameric channel. To test this prediction, the equilibrium among the four gating modes was quantified from the *f* histograms generated at different Gβγ concentrations, and the relative occupancy of each mode, $\Im_k$, was examined as a function of the parameter *P*. In each instance, this parameter was computed from the relative occupancy of mode 1, $\Im_1$, according to the equation $\Im_1 = 4P(1-P)^3/[1-(1-P)^4]$. This equilibrium analysis clearly indicated that the probability of observing each gating mode is binomially distributed as one would predict if the four Gβγ-binding sites are identical and independent. The structural basis for this functional equivalence of the Gβγ-binding sites in the heterotetrameric K_{ACh} channel remains to be determined. The NH_2- and COOH-terminal domains of both GIRK1 and GIRK4 bind Gβγ; however, the affinity of the COOH-terminal regions is different for the two subunits (Huang et al., 1997). In view of this fact, our data suggest that the GIRK1 and GIRK4 subunits must be arranged in a precise pattern to form the four equivalent Gβγ-binding sites, perhaps using Gβγ-binding blocks from both GIRK1 and GIRK4 polypeptide chains.

The probability of one of the four Gβγ-binding sites to be occupied, *P*, was a hyperbolic function of the Gβγ concentration (Fig. 8 *A*), and was well approximated by the equation:

$$P = P_{max}\,[G\beta\gamma]/([G\beta\gamma] + K_d), \qquad (2)$$

where K_d is the microscopic dissociation constant for Gβγ binding to the channel. The least-squares fit to the data provided a value of 0.63 for the parameter P_{max} and a K_d value of 1.29 nM. These values were used in Eqs. 1 and 2 to calculate the probability of observing each gating mode, P_k, as a function of the $G\beta_1\gamma_5$ concentration. Then from the P_k values and the experimentally determined open probability of the K_{ACh} channel in each gating mode ($P_{o1G\beta\gamma} = 0.0055 \pm 0.0006$, $P_{o2G\beta\gamma} = 0.0242 \pm 0.0015$, $P_{o3G\beta\gamma} = 0.0642 \pm 0.0048$, and $P_{o4G\beta\gamma} = 0.1409 \pm 0.0127$), we generated the theoretical stimulus–response curve for a K_{ACh} channel with four gating modes arising from the binding of a different number of Gβγ subunits to four equivalent and independent binding sites. The resulting curve (Fig. 8 *B, dotted line*) is sigmoidal, and its fit with the Hill equation,

$$R = R_{max}/\{1 + (k_d/[G\beta_1\gamma_5])^N\}, \qquad (3)$$

yields a Hill coefficient, *N*, of 1.2 and an apparent dissociation constant, k_d, of 2.71 nM. The theoretical and the experimental (Fig. 8 *B, solid line*) $G\beta_1\gamma_5$ concentration–response curves are identical in the concentration range 0.15–2.5 nM; however, at higher $G\beta_1\gamma_5$ concentrations, the theoretical curve approaches the saturation limit more gradually than the experimental curve (k_d of 1.09 nM and Hill coefficient of 1.73). This dis-

crepancy between the theoretical and the experimental curves can be explained by the desensitization of the K_{ACh} channel. We found that as $G\beta_1\gamma_5$ concentration was raised, the proportion of the blank data segments exceeded the probability of observing gating mode 0 (no $G\beta\gamma$ bound to the channel), P_o, calculated from Eq. 1. This behavior is expected if the K_{ACh} channel enters a desensitized state that depends on the $G\beta\gamma$ concentration. An additional possibility is that as the $G\beta\gamma$ concentration increases, the $G\beta_1\gamma_5$ dimers aggregate in the membrane and, consequently, the membrane concentration of $G\beta_1\gamma_5$ deviates from the one in the experimental chamber. Consistent with this possibility, the probability of $G\beta_1\gamma_5$ binding, P, saturated at P_{max} of 0.63 instead of reaching a value of 1. Perhaps a combination of these two factors suppresses the K_{ACh} channel responses at high $G\beta\gamma$ concentrations, and thus creates the steeper, switch-like stimulus–response curve observed in our experiments.

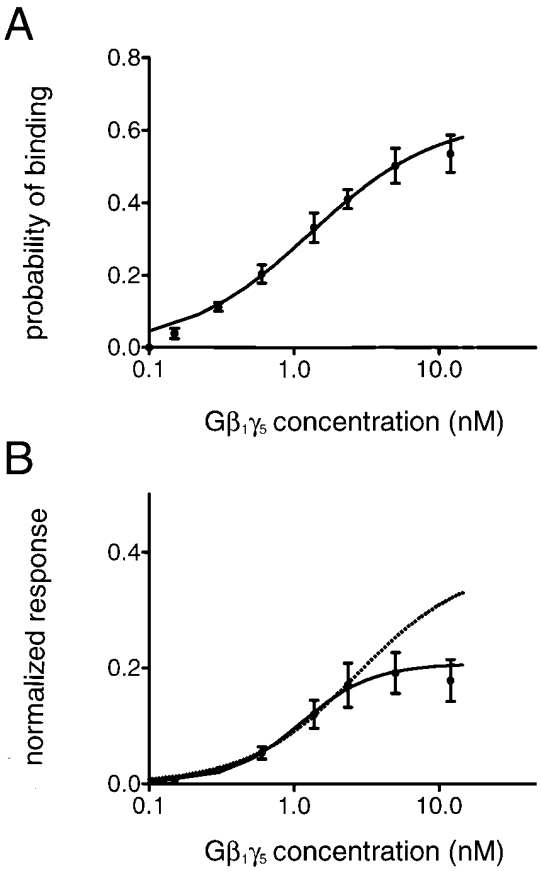

FIGURE 8. (*A*) $G\beta_1\gamma_5$ binding to the K_{ACh} channel. The probability of $G\beta_1\gamma_5$ binding, P, is plotted against $G\beta_1\gamma_5$ concentration. The points and error bars represent the mean ± SEM of three to five separate experiments. The solid line through the data represents the least-squares fit with a hyperbolic equation: $P = P_{max}[G\beta\gamma]/([G\beta\gamma] + K_d)$, with $P_{max} = 0.63$ and $K_d = 1.29$ nM. (*B*) $G\beta_1\gamma_5$-concentration dependence of the K_{ACh} channel activation. The steady state K_{ACh} channel open probability, P_o, is normalized to the open probability of mode 4, $P_{o4G\beta\gamma}$, determined in each experiment, and the $P_o/P_{o4G\beta\gamma}$ ratio is plotted against $G\beta_1\gamma_5$ concentration. Symbols and bars are mean ± SEM of three to five separate experiments. The continuous line represents the least-squares fit with the Hill equation (Eq. 3) and yields a Hill coefficient of 1.73 and an apparent k_d of 1.09 nM. The predicted $P_o/P_{o4G\beta\gamma}$ ratio for a K_{ACh} channel with four gating modes arising from the binding of a different number of $G\beta\gamma$ subunits to four binding sites in the channel structure (Eqs. 1 and 2) is plotted for comparison as a dotted line.

Physiological Relevance of Modal Regulation of the K_{ACh} Channel by $G\beta\gamma$

The $G\beta\gamma$-driven control of the modal prevalence is not only evolutionarily conserved in K_{ACh} channel regulation from frog to mammalian atrial myocytes, as demonstrated in the present study, but is also widespread and biologically versatile in other signaling systems. The same mechanism is encountered in the neurotransmitter-mediated downmodulation of neuronal N-type Ca^{2+} channels (Delcour and Tsien, 1993) and in the persistent activation of Na^+ channels in mammalian central neurons (Alzheimer et al., 1993; Ma et al., 1997). In both systems, the G protein $\beta\gamma$ subunits were implicated as the signal-relaying units that interact with these channels (Herlitze et al., 1996; Ikeda, 1996; Ma et al., 1997). The identity of the $G\beta\gamma$ subunits and the mechanism through which they accomplish the modal control may vary from one signaling cascade to another; still, in each case the existence of multiple functional states of the effector molecule helps to ensure the sensitivity and fidelity of $G\beta\gamma$-mediated signaling. In the case of the K_{ACh} channel, the type of regulation described here can be exploited in at least two different ways. The cell could downregulate the microscopic affinity of the K_{ACh} channel for $G\beta\gamma$, in which case the system would filter out small changes in the $G\beta\gamma$ concentration and yet allow the K_{ACh} channel to respond to sufficient changes in $G\beta\gamma$ concentration that occur upon stimulation of either m_2-muscarinic or A_1-purinergic receptors. Alternatively, the K_{ACh} channel affinity for $G\beta\gamma$ could be upregulated so that a small change in the $G\beta\gamma$ concentration could translate into a large response. The variability in the apparent affinity of the channel for $G\beta_1\gamma_5$ encountered in our experiments implies that the cell, indeed, regulates the sensitivity of the K_{ACh} channel to receptor stimulation. Recently, phosphatidylinositol 4,5-bisphosphate (PIP_2) was identified as one of the potential factors contributing to such regulation (Huang et al., 1998; Sui et al., 1998).

Sensitivity is only one of several important aspects of the behavior of a signaling system. Another is its specificity. In this aspect, a signaling molecule with multiple functional states like the K_{ACh} channel has the potential to filter out the "membrane noise" associated with the

G protein-mediated signaling. Activation of G proteins is a highly conserved signaling strategy used by a very large number of different G protein-coupled receptors colocalized in the cell membrane. Once the G proteins are activated and the Gβγ subunits are released, a heterogeneous population of Gβγ subunits is potentially available to act directly on the K_{ACh} channels. Under such circumstances, the specificity might arise from a differential ability of different Gβγ subunit combinations to activate the K_{ACh} channels. Studies with a limited number of purified recombinant Gβγ subunits, however, indicate that different Gβγ combinations activate the channel with comparable efficacies (Wickman et al., 1994). Thus, there might be additional mechanisms for ensuring the specificity of interactions between the expanding number of signaling partners. One attractive possibility is that the receptor, G protein, and the K_{ACh} channel exist as a precoupled complex (Huang et al., 1995). Based on present study, an additional mechanism, the presence of functional states of the K_{ACh} channel with very low open probabilities, is suggested. Such states would absorb some fraction of the Gβγ released in the membrane without producing substantial current through the channel, thus filtering small inputs from multiple membrane receptors.

We are grateful to Drs. Howard Morgan, Olaf Andersen, and the two reviewers for critical comments on the manuscript. We thank Dr. Mark Richardson for help with purification of $G\beta_1\gamma_5$ subunits, Tom Smink and Vivian Kalman for the expert technical assistance, and Holly Benscoter for artwork.

This work was supported by National Institutes of Health grant GM-39867 (J.D. Robishaw) and a Grant-In-Aid by the American Heart Association, Pennsylvania Affiliate (T.T. Ivanova-Nikolova).

Original version received 29 December 1997 and accepted version received 11 June 1998.

REFERENCES

Alzheimer, C., P.C. Schwindt, and W.E. Crill. 1993. Modal gating of Na^+ channels as a mechanism of persistent Na^+ current in pyramidal neurons from rat and cat sensorimotor cortex. *J. Neurosci.* 13:660–673.

Breitwieser, G.E., and G. Szabo. 1985. Uncoupling of cardiac muscarinic and β-adrenergic receptors from ion channels by a guanine nucleotide analogue. *Nature.* 317:538–540.

Clapham, D.E., and E.J. Neer. 1993. New roles for G-protein βγ-dimers in transmembrane signalling. *Nature.* 365:403–406.

Colquhoun, D., and A.G. Hawkes. 1981. On the stochastic properties of single ion channels. *Proc. R. Soc. Ser. B.* 211:205–235.

Colquhoun, D., and A.G. Hawkes. 1983. The principles of the stochastic interpretation of ion-channel mechanisms. *In* Single Channel Recording. B. Sakmann and E. Neher, editors. Plenum Publishing Corp., New York. 135–175.

Dascal, N., W. Schreibmayer, N.F. Lim, W. Wang, C. Chavkin, L. DiMagno, C. Labarca, B.L. Kieffer, C. Gaveriaux-Ruff, D. Trollinger, H.A. Lester, and N. Davidson. 1993. Atrial G protein-activated K^+ channel: expression cloning and molecular properties. *Proc. Natl. Acad. Sci. USA.* 90:10235–10239.

Dascal, N., C.A. Doupnik, T. Ivanina, S. Bausch, W. Wang, C. Lin, J. Garvey, C. Chavkin, H.A. Lester, and N. Davidson. 1995. Inhibition of function in *Xenopus* oocytes of the inwardly rectifying G-protein-activated atrial K^+ channel (GIRK1) by overexpression of a membrane-attached form of the C-terminal tail. *Proc. Natl. Acad. Sci. USA.* 92:6758–6762.

Delcour, A.H., and R.W. Tsien. 1993. Altered prevalence of gating modes in neurotransmitter inhibition of N-type calcium channels. *Science.* 259:980–984.

Doupnik, C.A., N. Davidson, and H.A. Lester. 1995. The inward rectifier potassium channel family. *Curr. Opin. Neurobiol.* 5:268–277.

Doupnik, C.A., N. Davidson, H.A. Lester, and P. Kofuji. 1997. RGS proteins reconstitute the rapid gating kinetics of Gβγ-activated inwardly rectifying K^+ channels. *Proc. Natl. Acad. Sci. USA.* 94: 10461–10466.

Foster, K.A., P.J. McDermott, and J.D. Robishaw. 1990. Expression of G proteins in rat cardiac myocytes: effect of KCl depolarization. *Am. J. Physiol.* 28:H432–H441.

Hamill, O.P., A. Marty, E. Neher, B. Sakmann, and F.J. Sigworth. 1981. Improved patch-clamp techniques for high-resolution current recording from cells and cell-free membrane patches. *Pflügers Arch.* 391:85–100.

Hansen, C.A., S.K. Joseph, and J.D. Robishaw. 1994. Ins 1,4,5-P_3 and Ca^{2+} signaling in quiescent neonatal cardiac myocytes. *Biochim. Biophys. Acta.* 1224:517–526.

Hansen, C.A., A.G. Schroering, and J.D. Robishaw. 1995. Subunit expression of signal transducing G proteins in cardiac tissue: implications for phospholipase C-β regulation. *J. Mol. Cell Cardiol.* 27:471–484.

Herlitze, S., D.E. Garcia, K. Mackie, B. Hille, T. Scheuer, and W.A. Catterall. 1996. Modulation of Ca^{2+} channels by G-protein βγ subunits. *Nature.* 380:258–262.

Hosoya, Y., M. Yamada, H. Ito, and Y. Kurachi. 1996. A functional model for G protein activation of the muscarinic K^+ channel in guinea pig atrial myocytes. *J. Gen. Physiol.* 108:485–495.

Huang, C.-L., P.A. Slesinger, P.J. Casey, Y.N. Jan, and L.Y. Jan. 1995. Evidence that direct binding of Gβγ to the GIRK1 G-protein-gated inwardly rectifying K^+ channels is important for channel activation. *Neuron.* 15:1133–1143.

Huang, C.-L., Y.N. Jan, and L.Y. Jan. 1997. Binding of the G protein βγ subunit to multiple regions of G protein-gated inward-rectifying K^+ channels. *FEBS Lett.* 405:291–298.

Huang, C.-L., S. Feng, and D.W. Hilgemann. 1998. Direct activation of inward rectifier potassium channels by PIP_2 and its stabilization by Gβγ. *Nature.* 391:803–806.

Ikeda, S. 1996. Voltage-dependent modulation of N-type calcium channels by G-protein βγ subunits. *Nature.* 380:255–258.

Iniguez-Lluhi, J.A., M.I. Simon, J.D. Robishaw, and A.G. Gilman. 1992. G protein βγ subunits synthesized in Sf9 cells. *J. Biol. Chem.* 267:23409–23417.

Ito, H., T. Sugimoto, I. Kobayashi, K. Takahashi, T. Katada, M. Ui,

and Y. Kurachi. 1991. On the mechanism of basal and agonist-induced activation of the G protein-gated muscarinic K^+ channel in atrial myocytes of guinea pig heart. *J. Gen. Physiol.* 98:517–533.

Ito, H., R.T. Tung, T. Sugimoto, I. Kobayashi, K. Takahashi, T. Katada, M. Ui, and Y. Kurachi. 1992. On the mechanism of G protein βγ subunit activation of the muscarinic K^+ channel in guinea pig atrial cell membrane. *J. Gen. Physiol.* 99:961–983.

Ivanova-Nikolova, T.T., and G.E. Breitwieser. 1997. Effector contributions to Gβγ-mediated signaling as revealed by muscarinic potassium channel gating. *J. Gen. Physiol.* 109:245–253.

Kozasa, T., and A.G. Gilman. 1995. Purification of recombinant G proteins from Sf9 cells by hexahistidine tagging of associated subunits. *J. Biol. Chem.* 270:1734–1741.

Krapivinsky, G., E.A. Gordon, K. Wickman, B. Velimirovic, L. Krapivinsky, and D.E. Clapham. 1995. The G-protein-gated atrial K^+ channel I_{KACh} is a heteromultimer of two inwardly rectifying K^+ channel proteins. *Nature.* 374:125–141.

Kubo, Y., E. Reuveny, P.A. Slesinger, Y.N. Jan, and L.Y. Jan. 1993. Primary structure and functional expression of a rat G-protein-coupled muscarinic potassium channel. *Nature.* 364:802–806.

Kunkel, M.T., and E.G. Peralta. 1995. Identification of domains conferring G protein regulation on inward rectifier potassium channels. *Cell.* 83:443–449.

Kurachi, Y. 1995. G protein regulation of cardiac muscarinic potassium channel. *Am. J. Physiol.* 269:C821–C830.

Lesage, F., F. Duprat, M. Fink, E. Guillemare, T. Coppola, M. Lazdunski, and J.P. Hugnot. 1994. Cloning provides evidence for a family of inward rectifier and G-protein coupled K^+ channels in the brain. *FEBS Lett.* 353:37–42.

Ma, J.Y., W.A. Catterall, and T. Scheuer. 1997. Persistent sodium currents through brain sodium channels induced by G protein βγ subunits. *Neuron.* 19:443–452.

Pfaffinger, P.J., J.M. Martin, D.D. Hunter, N.M. Nathanson, and B. Hille. 1985. GTP-binding proteins couple cardiac muscarinic receptors to a K channel. *Nature.* 317:536–538.

Reuveny, E., P.A. Slesinger, J. Inglese, J.M. Morales, J.A. Inigues-Lluhi, R.J. Lefkowitz, H.R. Bourne, Y.N. Jan, and L.Y. Jan. 1994. Activation of the cloned muscarinic potassium channel by G protein βγ subunits. *Nature.* 370:143–146.

Saitoh, O., Y. Kubo, Y. Miyatani, T. Asano, and H. Nakata. 1997. RGS8 accelerates G-protein-mediated modulation of K^+ currents. *Nature.* 390:525–529.

Silverman, S.K., H.A. Lester, and D.A. Dougherty. 1996. Subunit stoichiometry of a heteromultimeric G protein-coupled inward-rectifier K^+ channel. *J. Biol. Chem.* 266:19528–19535.

Soejima, M., and A. Noma. 1984. Mode of regulation of the ACh-sensitive K-channel by the muscarinic receptor in rabbit atrial cells. *Pflügers Arch.* 400:424–431.

Sui, J.L., J. Petit-Jacques, and D.E. Logothetis. 1998. Activation of the atrial K_{ACh} channel by the βγ subunits of G proteins or intracellular Na^+ ions depends on the presence of phosphatidylinositol phosphates. *Proc. Natl. Acad. Sci. USA.* 95:1307–1312.

Takao, K., M. Yoshii, A. Kanda, S. Kokubun, and T. Nukada. 1994. A region of the muscarinic-gated atrial K^+ channel critical for activation by G protein βγ subunits. *Neuron.* 13:747–755.

Tucker, S.J., M. Pessia, and J.P. Adelman. 1996. Muscarine-gated K^+ channel: subunit stoichiometry and structural domains essential for G protein stimulation. *Am. J. Physiol.* 271:H379–H385.

Wickman, K.D., J.A. Inigues-Lluhi, P.A. Davenport, R. Taussing, G.B. Krapivinsky, M.E. Linder, A.G. Gilman, and D.E. Clapham. 1994. Recombinant G-protein βγ subunits activate the muscarinic-gated atrial potassium channel. *Nature.* 368:255–257.

Wickman, K., J. Nemec, S.J. Gendler, and D.E. Clapham. 1998. Abnormal heart rate regulation in *GIRK4* knockout mice. *Neuron.* 20:103–114.